

Available online at [www.synsint.com](http://www.synsint.com)

Synthesis and Sintering

ISSN 2564-0186 (Print), ISSN 2564-0194 (Online)



Research article

# Synthesis of magnetite-silica-carbon quantum dot nanocomposites for melatonin drug delivery



A. Faeghinia , Hossein Nuranian \*, Mojtaba Eslami

Ceramics Department, Materials and Energy Research Center (MERC), P.O. Box 31779-83634, Karaj, Iran

## ABSTRACT

In targeted drug delivery, the drug is released at a specific and desired point and condition. In this research, magnetite cores (high saturation magnetization property ( $\text{emu.g}^{-1}59$ )) were used to target the drug system. First, magnetite nanoparticles were synthesized by the coprecipitation method from divalent and trivalent chloride salts of iron ( $\text{FeCl}_2$  and  $\text{FeCl}_3$ ), then mesoporous silicas (with a pore diameter of 13 nm) were formed by Stöber's method from the tetraethylorthosilicate (TEOS) silica source on magnetite cores in spheres form. After that, the carbon quantum dots were synthesized by hydrothermal method from citric acid, and their surface was immobilized by dimethylamine which was placed in silica cavities by physical adsorption method.

The effective drug melatonin (6.46 mg of melatonin per 100 mg of the drug system) was also loaded on this system by physical absorption method and the release of this drug was carefully determined by the release from the dialysis bag in the simulated environment of blood and cancer tissue. The quantum gain of the system was determined to be about 40%. The results showed that the loading of melatonin drug and carbon quantum dots was done well on silica nanoparticles with magnetite cores, and this system releases 30% of the drug even under temperature conditions.

© 2023 The Authors. Published by Synsint Research Group.

## KEYWORDS

Melatonin  
Silica  
Magnetic particles  
Drug delivery  
Synthesis



## 1. Introduction

This research is devoted to building a targeted and traceable drug delivery system and uses the melatonin hormone as a loaded drug. The melatonin hormone has a wide range of applications in the human body and it has positive and significant effects in the treatment of cancer and countless diseases. Recently, it has attracted a lot of comments.

The role of magnetite nanoparticles as drug delivery carriers is more pronounced due to having unique properties in comparison to the usual properties of other nanomaterials. These nanoparticles have the potential to revolutionize clinical diagnosis and treatment due to unique properties such as enhanced magnetic and superparamagnetic impulses, as well as the power of biological interactions at the cellular and

molecular levels, simple separation with the magnetic field, availability, and cheapness [1].

These properties lead to the easy application of these nanoparticles with the help of an external magnetic field and more absorption by the target tissue, and as a result more effective treatment in optimal therapeutic doses. The design of magnetic drug delivery systems needs to consider many factors, for example, magnetic properties and particle size, magnetic field strength, the capacity of the drug being loaded, the possibility of access to the target tissue, or the amount of effective presence in the bloodstream [2].

Due to their desirable properties, magnetite nanoparticles are the only type of nanoparticles approved by the Ministry of Health and Nutrition for therapeutic use [3]. Magnetite nanoparticles are obtained by one-step synthesis by alkaline co-precipitation method from divalent and

\* Corresponding author. E-mail address: [h.nouranian@merc.ac.ir](mailto:h.nouranian@merc.ac.ir) (H. Nuranian)

Received 24 February 2023; Received in revised form 17 April 2023; Accepted 18 April 2023.

Peer review under responsibility of Synsint Research Group. This is an open access article under the CC BY license (<https://creativecommons.org/licenses/by/4.0/>).  
<https://doi.org/10.53063/synsint.2023.32142>

trivalent iron salts. Chemical stability in physiological conditions and the possibility of chemical changes by applying different coatings on iron oxide core are the valuable properties of these particles [2].

In normal conditions, the surface of nanoparticles is easily oxidized, which strongly affects their properties. Different methods of protection and covering are used to prevent unwanted oxidation. By applying the coating, the amount of repulsive forces is increased and accumulation is prevented. Carbon, silica, metal, metal oxide, organic polymers, and surface active materials are among them [4].

Generally, carbon quantum dots contain many carboxylic acid groups on their surface, and for this reason, they have excellent solubility in water and are suitable for being acted upon by a variety of organic, polymeric, inorganic, or biological species [4]. Therefore, it is possible to design complex catalytic systems, based on carbon quantum dots, for the effective, useful, and cost-effective use of the entire spectrum of solar light. This is not possible in larger particle sizes and the fluorescence property is not observed either. Also, since the size of carbon nanoparticles is less than 10 nm, the catalytic property increases due to higher specific surface area [5].

Chen and colleagues conjugated CdTe quantum dots with Fe<sub>3</sub>O<sub>4</sub>-filled carbon nanotubes (CNTs) for the first time to develop a specific and novel nanopatform for magnetically guided drug delivery and optical imaging. Magnetically guided delivery was facilitated by filling Fe<sub>3</sub>O<sub>4</sub> into the CNTs, and as a result, the synergistic targeting performance was improved. Compared with nanocrystals immobilized on the outer surface of carbon nanotubes, the nanocrystals of magnetite inside carbon nanotubes increase its chemical stability, protect it from aggregating, and improve the capacity of drug loading [5].

In bottom-up synthesis methods such as combustion oxidation methods, hydrothermal, microwave, ultrasound, and chemical reactions, non-graphite carbon sources can be converted into graphite nanoparticles. These carbon quantum dots are luminescent and can be obtained from biocompatible sources [6–9].

Melatonin has a very wide range of effects and is one of the key hormones of the mammalian body. Almost all cells of the body have melatonin receptors, and melatonin has a special role in each part and organ [10].

The activation of melatonin receptors causes the prevention of fatal diseases by increasing the release of some cytokines that inhibit the immune system due to stress. The thymus is one of the target tissues of melatonin, and the destruction and reduction of its cells with increasing age is one of the reasons for reducing the ability of the immune system in old age. Many recent researches have shown that the change of seasons affects the functioning of the immune system, and melatonin plays an important role in this regard as well [11].

Melatonin is stronger than vitamin E, mannitol, glutathione and twice as efficient as strolax for cleaning free radicals caused by the oxidation of unsaturated fatty acids. The production and release of most hormones shows a time pattern or a 24-hour period, and lifestyle factors such as night shift work and sleep disorders, or using television or computers or mobile phones until midnight, or contact with agents. Especially, such as light at night, which disrupts the circadian rhythm, causes changes in the function of endocrine glands and changes the regulation of reproductive hormones, which is usually lead to the hormone-related diseases, such as breast cancer or prostate cancer [12]. Removal of the increases tumor growth and melatonin consumption reverses this effect and inhibits tumorigenesis caused by carcinogens. Melatonin reduces the growth of tumor cells by inhibiting mitosis and

regulating the activity of receptors in tumor cells [13]. In a research, it was observed that by adding melatonin to tamoxifen, the spread of the disease slowed down [14].

In another study, the consumption of high doses of melatonin (700 mg per day) had a transient decrease in the size of some tumor masses. Also, it is said that adding melatonin to chemotherapy and radiotherapy reduces the damage of blood cells and makes the treatment more tolerable. Research has shown that serum and urine melatonin levels in women with breast cancer are low, and melatonin administration inhibits the growth of breast tumors [13].

In research conducted by Li et al. MLT-loaded SiO<sub>2</sub> and MLT-loaded SiO<sub>2</sub> coated with HP55 (MLT-SiO<sub>2</sub>-HP55) nanosphere were obtained by adsorption in acetone solution and desolvation, respectively. The loading of MLT was observed mostly in the SiO<sub>2</sub> pores. In contrast, a large part of MLT-SiO<sub>2</sub> was covered by HP55 coating. Characterization showed that the release rate of raw MLT in the simulated gastric fluid was dramatically lower than that of MLT from MLT-SiO<sub>2</sub> [6].

Also, in another study, Zarazhowski and Sena showed how carbon quantum dots are effective in modern drug delivery and drug loading, and medical imaging and can open new horizons in drug delivery and diagnostic applications [13].

Melatonin reduces the growth of tumor cells by inhibiting mitosis and regulating the activity of receptors in tumor cells [15]. In a research, it was observed that by adding melatonin to tamoxifen, the spread of the disease slowed down. In another study, the consumption of high doses of melatonin (700 mg per day) had a transient decrease in the size of some tumor masses. Also, it is said that adding melatonin to chemotherapy and radiotherapy reduces the damage of blood cells and makes the treatment more tolerable [15].

The aim of this research was to develop one of the most important and widely used drug carriers in chemotherapy and targeted drug delivery and to add better tracking capabilities to observe the penetration and effect of the drug on the desired tissue. The present work is the use of carbon quantum dots together with porous silica and magnetite (three actions) together to investigate the release of melatonin as an anti-cancer drug. Previously, this drug has not been loaded on this system. In previous research, only magnetite particles were used to release this drug, but in the present work, carbon dots can facilitate the detection of the drug due to its fluorescent properties. Also, this system was checked with the drug melatonin, which researchers believe can play a useful role in fighting cancer, and the way this drug is released.

---

## 2. Experimental Procedure

### 2.1. Synthesis of magnetite Fe<sub>3</sub>O<sub>4</sub> nanoparticles

In co-precipitation method, for the synthesis of magnetite nanoparticles, divalent iron chloride salts were used as iron source and deionized water as solvent. In order to obtain a transparent and uniform orange solution, the temperature of the ultrasonic bath was increased to 75 °C.

0.01 M sodium hydroxide solution was added drop by drop to the contents of the flask for 100 minutes. The balloon contents were centrifuged at 4000 rpm and coarse particles were separated from it, magnetite nanoparticles were collected using a strong neodymium magnet and washed several times with deionized water and ethanol and finally, it was dried in a vacuum oven at 50 °C for 24 hours. The dried powder is black and cloudy.

## 2.2. Synthesis of silica on magnetite cores

Stöber's method was used for the synthesis of silica nanoparticles on magnetite cores. 2 grams of  $\text{Fe}_3\text{O}_4$  powder was transferred to a 500 ml flask with 200 ml of ethanol, and by stirring for half an hour under ultrasonic waves, the magnetite nanoparticles were completely dispersed. Then 5 ml of ammonia and 4 ml of tetraethylorthosilicate were added to 30 ml of ethanol. This solution was added drop by drop using a burette, for 1 hour, to the solution containing magnetite nanoparticles, in a 500 ml flask, under ultrasonic waves. The resulting mixture was stirred for 24 hours by an incubator at a speed of 150 rpm. The above operation was carried out at room temperature and the precipitate was washed several times with deionized water and ethanol, and after centrifugation at 4000 rpm for 24 hours, it was dried in an oven at a temperature of 60 °C.

## 2.3. Synthesis of carbon quantum dots

The bottom-up hydrothermal method was used for the synthesis of carbon quantum dots. To increase the quantum yield of carbon dots, surface modification was used by making the surface of carbon quantum dots ineffective by functional groups. In this way, different precursors containing carbon and precursors containing functional groups were added and dispersed in 25 cc of deionized water, then it was transferred to the autoclave and at different times for 2–5 hours in the oven at 180–250 °C and finally their fluorescence intensity was compared under UV radiation with 252 and 352 nm wavelengths.

For the synthesis of carbon quantum dots, the hydrothermal synthesis of citric acid with diethylamine was used, which had quantum yield and suitable conditions, and its product was used to load the drug delivery system discussed in this research. For this purpose, 25 cc of acid one molar citric acid was poured into the autoclave along with 2 cc of diethylamine, and the autoclave was placed at 200 °C for 3 hours. The resulting product was centrifuged 5 times at 15000 rpm for 15 minutes each time. This product emits blue color under UV rays with a wavelength of 350 nm.

## 2.4. Loading carbon quantum dots on magnetite cores with silica coating

To load the carbon dots on this drug delivery system, 200 mg of magnetite cores that were coated with silica by Stöber's method were added to 5 cc of deionized water and subjected to ultrasonic until they were completely dispersed, then 2 cc of solution of the obtained carbon dots were added to the above suspension and the final suspension was placed on the incubator at a speed of 240 rpm for 24 hours. After 24 hours, the suspension was washed several times with deionized water and dried at 50 °C under vacuum for 8 hours. The important and significant point in this loading is to activate the silica, so that, before the loading operation, the magnetic cores covered with silica should be placed in a vacuum environment for 6 hours, until the porous silica is emptied of air and ready to be loaded.

The nitrogen absorption/desorption test was performed to investigate the surface porosity of the magnetite/silica nanocomposite, this test was performed at a temperature of 77 K, and the curve obtained from nitrogen absorption and desorption, as seen in Fig. 1, is the fourth type curve and it is related to porous materials. In this test, the volume of pores on the porous surface of the synthesized nanoparticles was calculated to be 42  $\text{cm}^3/\text{g}$  and the specific surface area of these

nanoparticles is 86  $\text{m}^2/\text{g}$ . The average diameter of the holes on the surface of these magnetite/silica nanoparticles, as can be seen in Fig. 1, is 13 nm and shows that the surface of these nanoparticles is mesoporous.

## 2.5. Loading of melatonin on magnetite/silica/carbon quantum dots drug delivery system

To load melatonin on the discussed drug delivery system, 80 mg of melatonin dry powder was dispersed in 2 cc of acetone by a magnetic stirrer. Also, 100 mg of the obtained pharmaceutical system was dispersed in 4 cc of acetone under ultrasonic waves, the solution containing melatonin was added to it, and the container was transferred to the incubator to be stirred for 1 hour at a speed of 250 rpm. Then the drug delivery system was centrifuged to separate the slag solution containing melatonin to calculate the amount of drug loaded and then the system was washed with acetone and finally dried at 50 °C for 10 hours.

It should be noted that before loading the drug, the drug delivery system was placed in a vacuum environment for 12 hours to activate, and this operation was carried out at room temperature.

## 2.6. Drug release in the laboratory environment

In order to check the drug delivery of the prepared drug delivery system, the method of dissolution test and dialysis bag was done at 40 °C (cancer tissue temperature) and pH 6 (cancer tissue pH). After placing 28 mg of the melatonin-loaded drug system in the dialysis bag, the dialysis bag was placed in a dark environment and in a container containing buffer. The container was transferred to the incubator at a speed of 40 rpm at specified times, 2 cc of the buffer medium was removed and 2 cc of buffer, with the same pH as the solvent medium, was added to it.

These samples were taken at 15, 30, 60, 90, 120, 180, 240, 300, 420, 540, 600, 720, 840, 960, 1200, 1420, 1740, 3480, 5200, and 7200 minutes. The optical absorption of the removed samples was checked by UV-Vis optical spectrometer with a wavelength of 199 nm. After that, the dilution resulting from the

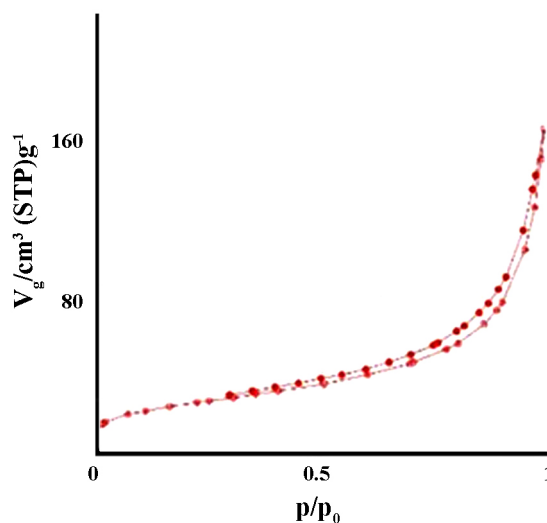


Fig. 1. The pores diameter of nano porous  $\text{Fe}_3\text{O}_4/\text{SiO}_2$  composite surface.

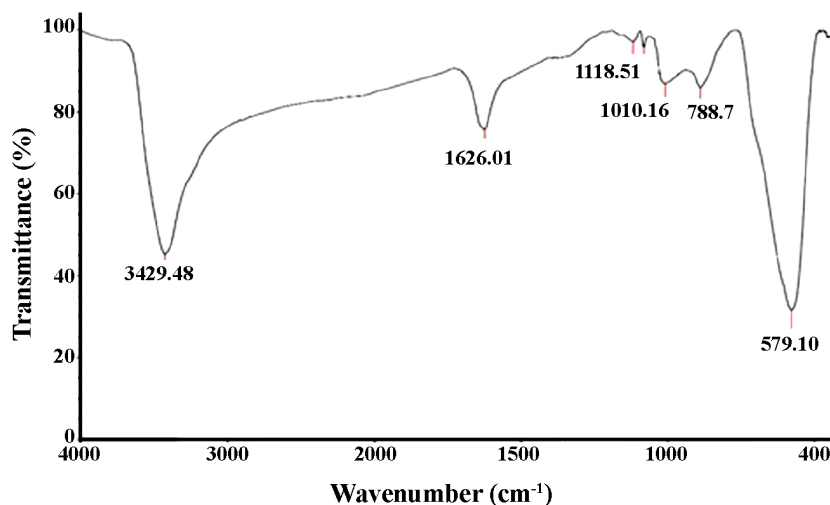


Fig. 2. The FT-IR result of drug delivery MNP/MSN/CQD system.

increase in volume and decrease of a certain concentration of the sample occurs. Eq. 1 was used to express the concentrations of the solution at each moment and then the concentration curve was released. The drug delivery was plotted vs. time, and the concentration and release rate of the drug were checked from the plotted curves. In this equation,  $c$  is the sample concentration at any time and  $C$  is the concentration measured by UV and  $v$  is the volume removed from the environment equal to 2 cc and  $V$  is the total sample volume equal to 20 cc and  $s$  is the number of samples removed [16].

$$C = C + v/V \sum_{s=1}^{n-1} c \quad (1)$$

### 2.7. Selection of UV-Vis wavelength

The amount of drug was measured at 199 nm wavelength. The 199 nm wavelength was chosen based on the absorption peak in the UV-Vis test corresponding to this wavelength. The released concentration of the drug was determined by the equation of the line obtained from the calibration curve specific to that environment. The reason for using ultraviolet-visible measurement was the ease and availability of the corresponding device compared to other analytical methods. The existence of double and hydrogen bonding groups in drugs gives them the

characteristic to be easily measured by the ultraviolet absorption method.

## 3. Results and discussion

### 3.1. Characterization of the drug system of magnetite/silica/carbon quantum dots nanocomposite

Fig. 2 corresponded to the results of FT-IR analysis of magnetite/silica/carbon quantum dot samples. In the spectroscopic diagram, the peak in the range of 1000–1300  $\text{cm}^{-1}$  relates to C–O group bonds, the peak corresponding to 3429  $\text{cm}^{-1}$  relates to the bonds of the carboxylic group on the surface of carbon quantum dots, and the average peak in the area of 1626  $\text{cm}^{-1}$  relates to stretching vibrations of C–C bonds, which indicates the presence of carbon quantum dots in the composition.

### 3.2. Properties of magnetite/silica/carbon quantum dots/melatonin magnetic nanocomposite

Since in this research targeting the drug carrier was the reason for using magnetic nanoparticles, it is very important and necessary to determine the magnetic properties of these nanoparticles. A vibrating sample

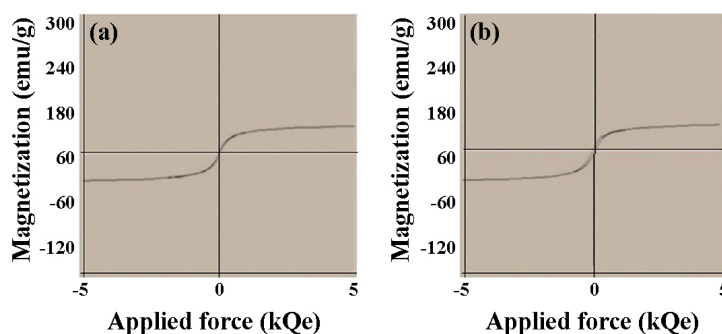


Fig. 3. The VSM results of a) the MNP/MSN/CQD/MLT and b) the magnetite/silica core.

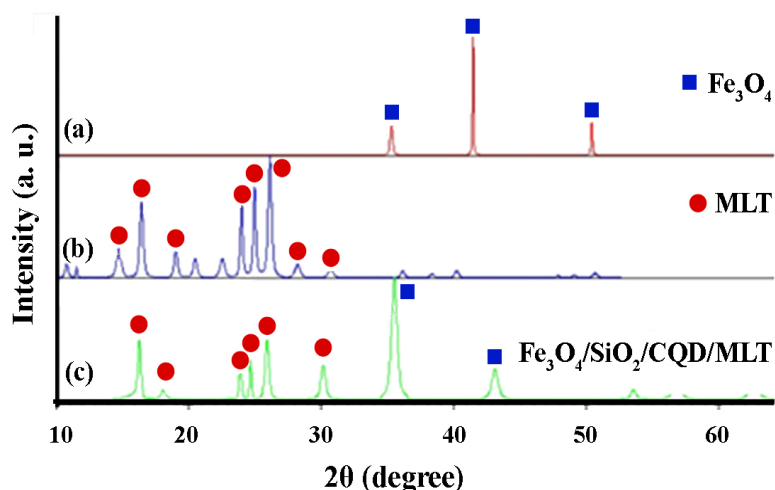


Fig. 4. The XRD patterns of a) magnetite, b) melatonin, and c) the loaded drug delivery MNP/MSN/CQD/MLT system.

magnetometer was used to determine the magnetization of nanoparticles. VSM curve of magnetite/silica nanocomposite was shown in Fig. 3. The magnetization of these particles has decreased slightly compared to magnetite cores, which was predictable due to the non-magnetism of silica.

In the magnetic ferrites of the spinel structure, if the magnetic cations, such as iron, are replaced by non-magnetic cations, which tend to be placed in the tetrahedral space, in this case, the magnetic properties of the material change [17].

By reducing the concentration of magnetic ions, disruption of the order of spins causes the instability of the magnetic order and affects the anisotropy of the magneto crystal, and this leads to the reduction of the residual field and affects the hysteresis losses [17]. This value is  $59 \text{ emu.g}^{-1}$ , which is suitable and sufficient for medical applications. On the other hand, in the magnetite/silica nanocomposite, there is no trace of magnetic remanence and it can be concluded that this nanocomposite is superparamagnetic.

### 3.3. Investigation of the crystal structure of magnetite/silica/carbon quantum dot/melatonin

The peaks related to the synthesized magnetite nanoparticles were detected by the Expert software database. The synthesized nanoparticles correspond to the magnetite reference sample with card number 01-086-1337 crystallized in the spinel cubic structure. This is a single-phase structure without any impurities. In terms of symmetry, the unit cell is placed in space group  $fd3m$ .

The obtained XRD pattern of the loaded drug delivery system shows their correspondence with the pattern of the magnetite/silica/carbon dots drug delivery system and the XRD pattern of melatonin. The loading of this drug on the discussed drug delivery system has been successful. In Fig. 4, the correspondence between these 3 analyzes can be seen.

No evidence related to the presence of impurity was observed in the XRD pattern. It is observed that the peaks of the synthesized sample are wider, which indicates the very small size of the nanoparticles. The crystal size was calculated to be 20 nm using the Debye-Scherrer equation.

### 3.4. Determination of photoluminescence emission

Carbon quantum dots usually show obvious light absorption in the ultraviolet region, extending into the visible range. The intense band in the region of 250–300 nm, which exists in the carbon quantum dots, is known as the transition peak. Surface functional groups also play an important role in determining the absorption wavelength of carbon dots. For example, the absorption band of carbon dots increases to longer wavelengths after being functionalized with amine groups (such as ammonia or 4,7,10-trioxa-1,13-tridecanediamine or organosilanes). To investigate the luminescence response of the loaded drug delivery system, photoluminescence spectroscopy was used. For this purpose, two wavelengths of 350 and 320 nm were used to excite the sample, and as can be seen in Fig. 5, the emission with the excitation wave of 320 nm has better results and shows the intense emission in the wavelengths of 440–460 nm.

The study of the optical properties of carbon nanodots is based on their photoluminescence mechanisms, which are directly related to the method of synthesis and functionalization of their surface. Two main photoluminescence mechanisms of carbon nanodots are related to surface energy traps and quantum size effect [18]. Blue emission (at shorter wavelengths) is due to the quantum size effect, while green emission (at longer wavelengths) is due to surface energy traps.

It is well known that carbon nanodots with small sizes of 1.2 nm have emission in the ultraviolet region, while with medium sizes from 1.5 to 3 nm in the visible light region and carbon nanodots with large sizes of 3.8 nm emit in the near-infrared region [18]. The photoluminescence emission spectrum of the loaded drug system in the violet range can be the reason for the presence of carbon dots with a particle size of 1.5 to 3 nm.

### 3.5. Determination of morphology and size

According to the SEM micrograph in Fig. 6, the size of the loaded drug delivery system particles is less than 100 nm, suitable and practical for medical applications and penetration and maintenance. The size of the nanoparticles was between 20 and 60 nm.

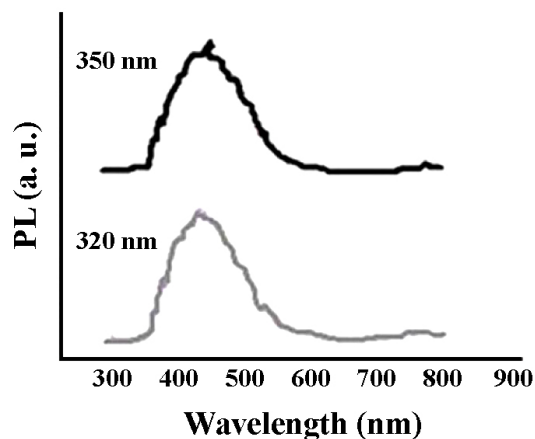


Fig. 5. The photoluminescence results of loaded drug delivery system.

This image confirms the uniform morphology and almost spherical shape. The presence of some larger particles is due to the condensation or overlapping of some smaller particles during the preparation and drying stage. In this part, it can be seen that the size of the particles corresponds almost to the size of the crystal obtained by XRD.

The way particles are placed next to each other is such that a certain number of particles stick together and create clusters. The clusters created here have close dimensions and the size of these clusters is all below 100 nm. In applications such as MRI and hyperthermia, it is necessary that the average size of nanomaterials does not exceed a critical limit.

With the increase in the size of the particles, the speed of their clearance from the bloodstream by the immune system increases [19].

### 3.6. Qualitative review of functional groups

Fig. 7 shows the spectroscopic results of the loaded system discussed in this research. The peak in the area of  $3304\text{ cm}^{-1}$  is related to the stretching vibrations of the N–H bond, and the peak in the area of

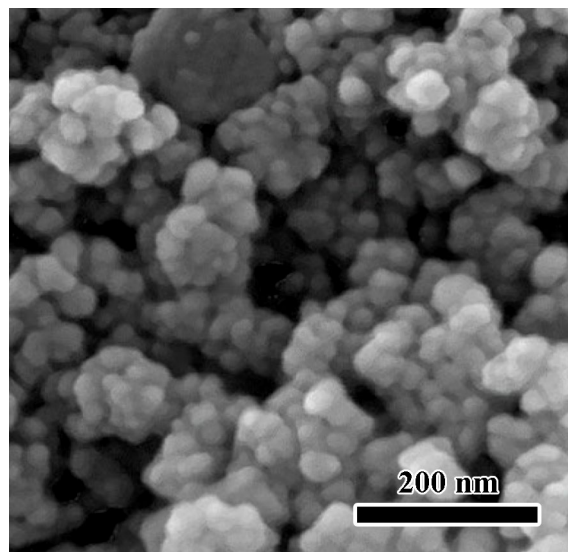


Fig. 6. The SEM micrograph of MNP/MSN/CQD/MLT loaded drug delivery system particles.

$2928\text{ cm}^{-1}$  is related to the stretching vibrations of the C–H bond. The peaks corresponding to the  $1200\text{--}1370\text{ cm}^{-1}$  region belong to the vibrations of C–N bonds in melatonin, and the peak corresponding to the  $1555\text{ cm}^{-1}$  region is related to the C=C double bond in the aromatic rings in the melatonin compound. The peak corresponding to  $1112\text{ cm}^{-1}$  is related to the stretching vibrations of the C–O bond. The FTIR pattern obtained from the loaded pharmaceutical system confirms the presence of carbon quantum dots and melatonin in the composition.

By comparing the position shift of the  $570\text{ cm}^{-1}$  band, it was detected that the loaded sample has a slight shift towards the lower wave number. This band is related to the tetrahedral position of the magnetite complex groups, which, with a slight change in the composition, and change in the length of the cation-oxygen bond, this position can be caused by the entering of silica into the magnetite structure.

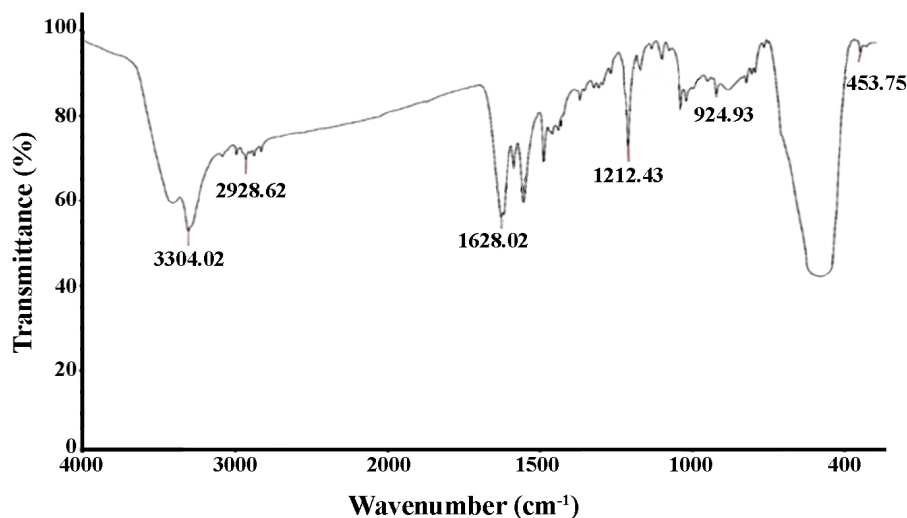


Fig. 7. The FT-IR pattern of drug delivery system of MNP/MSN/CQD/MLT.

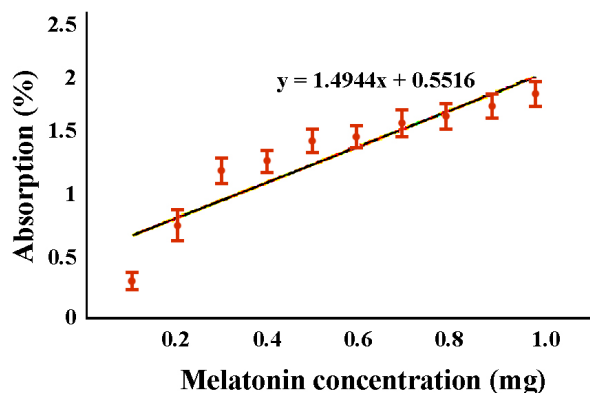


Fig. 8. The calibration curve for drug concentration determination.

### 3.7. Examining the release rate of the drug release test in the laboratory environment

Determination of instantaneous concentration with calibration curve was done. The calibration curve was used to determine the total amount of melatonin and its amount in the drug release phase. The calibration curve was drawn as follows. Inside 10 microtubes of 2 ml, which are numbered from 1 to 10, the values are 0.1, 0.2, 0.3, 0.4, 0.5, 0.6, 0.7, 0.8, 0.9, and 1 mg of the effective drug melatonin were placed in the microtube and the remaining volume of the microtube was adjusted to pH 7 with phosphate buffer solution. After complete dissolution of the drug in the buffer, the absorbance of each solution was recorded at 199 nm. Fig. 8 is the calibration curve and shows the changes in absorbance in terms of concentration, based on the figure, the equation of the absorbance line was obtained linearly vs. concentration, where  $x$  gives the concentration and  $y$  gives the amount of absorbance.

The amount of drug loaded on the drug delivery system was calculated to be 7.661 mg per 100 mg of the system.

$$y = 1.4944x + 0.5516 \quad (2)$$

### 3.8. Release of melatonin at pH 7.4 and environment without light

In order to measure the release rate of melatonin from the synthesized system, 28 mg of the loaded system was dispersed in 2 cc of deionized

water by ultrasonic waves, and the resulting black liquid was transferred to the dialysis bag. Dialysis was placed in 30 cc of buffer with pH = 7.4. At this stage of the experiment, at different times, 2 ml samples were taken from the test medium and replaced with fresh buffer, so that the volume of the solution remained 30 cc.

The optical absorbance of the samples was analyzed by Vis-UV. The concentration change due to volume increase was corrected by the equation. The drug release curve can be seen in Fig. 9. Based on the results obtained from the optimization of this drug delivery system, the initial sudden release of 23% of the loaded drug occurred in the first three hours, and then with a total decrease of 33% of the drug gradient, during the remaining 10 hours, melatonin was released from the synthetic system.

In a drug release system, in addition to the optimal loading of the drug, its release behavior is also very important, and it is desirable to achieve continuous and stable drug release in a controlled time. The drug release probability depends on the structure of the drug and the morphology of the carrier and its surface chemistry [20, 21]. Therefore, there are different drug release mechanisms. The profile shown in Fig. 9 shows that the release of melatonin drug from the carriers follows the Sigmoid Hill model. The Hill model includes three regions the initial (delayed) phase, the explosive phase, and the saturation phase. The existence of the initial phase and its length depend on the strength and intensity of the interaction between the drug and the carrier.

It can be seen that melatonin is released in a simulated cell tissue

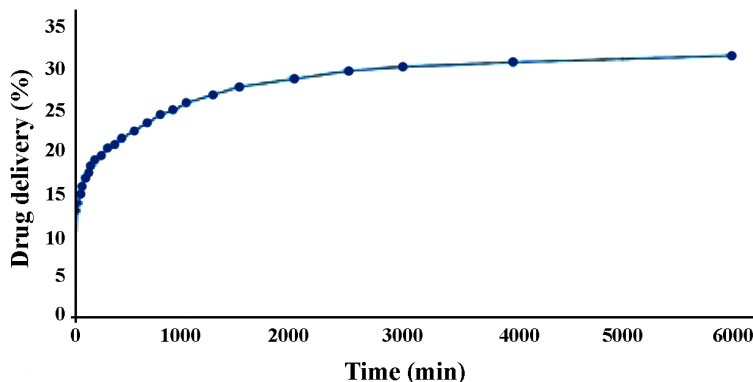


Fig. 9. The melatonin drug delivery in the pH of the blood.

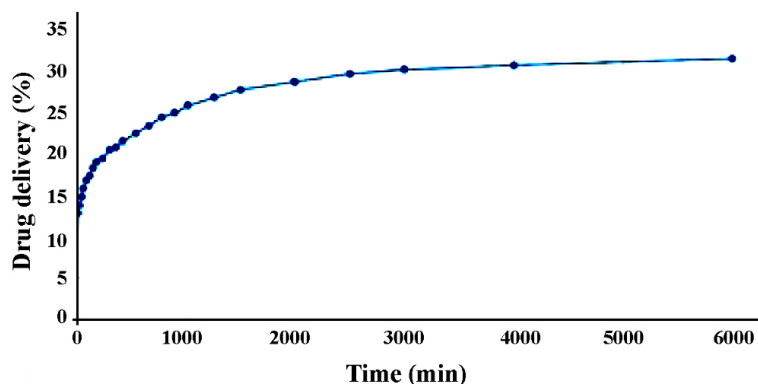


Fig. 10. The melatonin drug delivery in the pH of the cell tissue at the 40 °C.

environment with pH 6 and 40 °C and a dark environment. In this step, buffer sampling was done at 40 °C and in a dark environment at different times, and 2 ml samples were taken from the test medium and replaced with a fresh buffer so that the volume of the buffer solution remained at 30 cc. The optical absorbance of the samples was obtained by Vis-UV. The concentration change due to volume increase was corrected by the equation [22–24]. The drug release values from the synthesized nanocomposite can be seen in Fig. 10.

By comparing the results of Figs. 9 and 10, it can be seen that the percentage of drug release in cancer tissue after 1000 minutes is 35% by volume, and the drug release is 25% in the blood environment. This issue means that the drug has fewer side effects due to the longer release time in the blood.

#### 4. Conclusions

The obtained system had good load ability to the drug melatonin, which was calculated as 6.46 mg of melatonin per 100 mg of the discussed drug system. Also, the loading of carbon quantum dots is well done on it. This system showed good characteristics in the tests conducted in this research.

Features such as suitable particle size (below 100 nm), mesoporous surface (average size of holes 13 nm), suitable dispersibility, high specific surface area (86 m<sup>2</sup>/g), high saturation magnetization property (59 emu.g<sup>-1</sup>), and the superparamagnetism (zero magnetic residuum), the ability to simultaneously load carbon quantum dots and melatonin, the drug release ability in blood and cancer tissue, are the importance of continuing the discussion and research on this system. Cell toxicity and clinical tests on cell culture medium, TEM photography, and imaging of the process of penetration of the system into the cell by fluorescence microscope can help to better understand this system and its applications.

#### CRedit authorship contribution statement

**A. Faeghinia:** Writing – original draft, Conceptualization, Funding acquisition, Investigation.

**Hossein Nuranian:** Methodology, Project administration, Resources, Writing – review & editing.

**Mojtaba Eslami:** Data curation, Formal Analysis, Visualization.

#### Data availability

The data underlying this article will be shared on reasonable request to the corresponding author.

#### Declaration of competing interest

The authors declare no competing interests.

#### Funding and acknowledgment

The authors gratefully acknowledge the generous financial support provided by the Materials and Energy Research Center, under the Coating Project with Contract No. 371397057. This funding played a pivotal role in the successful execution of the research, and the authors are sincerely thankful for their contribution to this work.

#### References

- [1] N. Khan, F. Afaq, H. Mukhtar, Lifestyle as risk factor for cancer: Evidence from human studies, *Cancer Lett.* 293 (2010) 133–143. <https://doi.org/10.1016/j.canlet.2009.12.013>.
- [2] N.G. Zaorsky, T.M. Churilla, B.L. Egleston, S.G. Fisher, J.A. Ridge, et al., Causes of death among cancer patients, *Ann. Oncol.* 28 (2017) 400–407. <https://doi.org/10.1093/annonc/mdw604>.
- [3] R. Narayan, U.Y. Nayak, A.M. Raichur, S. Garg, Mesoporous silica nanoparticles: A comprehensive review on synthesis and recent advances, *Pharmaceutics*. 10 (2018) 1–49. <https://doi.org/10.3390/pharmaceutics10030118>.
- [4] L. Shen, B. Li, Y. Qiao, Fe<sub>3</sub>O<sub>4</sub> nanoparticles in targeted drug/gene delivery systems, *Materials (Basel)*. 11 (2018) 1–29. <https://doi.org/10.3390/ma11020324>.
- [5] M.L. Chen, Y. J. He, X. W. Chen, J. H. Wang, Quantum dots conjugated with Fe<sub>3</sub>O<sub>4</sub>-filled carbon nanotubes for cancer-targeted imaging and magnetically guided drug delivery, *Langmuir*. 28 (2012) 16469–16476. <https://doi.org/10.1021/la303957y>.
- [6] A. Yadegari, J. Khezri, S. Esfandiari, H. Mahdavi, A.A. Karkhane, et al., Bottom-up synthesis of nitrogen and oxygen co-decorated carbon quantum dots with enhanced DNA plasmid expression, *Colloids Surf. B*. 184 (2019) 110543. <https://doi.org/10.1016/j.colsurfb.2019.110543>.
- [7] D.-R. Hang, D.-Y. Sun, C.-H. Chen, H.-F. Wu, M.-S. Chou, et al., Facile Bottom-up Preparation of WS<sub>2</sub>-Based Water-Soluble Quantum Dots as Luminescent Probes for Hydrogen Peroxide and

- Glucose, *Nanoscale Res. Lett.* 14 (2019) 271. <https://doi.org/10.1186/s11671-019-3109-5>.
- [8] I.-A. Baragau, N.P. Power, D.J. Morgan, T. Heil, R.A. Lobo, et al., Continuous hydrothermal flow synthesis of blue-luminescent, excitation-independent nitrogen-doped carbon quantum dots as nanosensors, *J. Mater. Chem. A* 8 (2020) 3270–3279. <https://doi.org/10.1039/C9TA11781D>.
- [9] P. Rawat, P. Nain, S. Sharma, P.K. Sharma, V. Malik, et al., An overview of synthetic methods and applications of photoluminescence properties of carbon quantum dots, *Luminescence* 38 (2023) 845–866. <https://doi.org/10.1002/bio.4255>.
- [10] Y. Li, S.Li, Y. Zhou, X. Meng, J.-J. Zhang, et al., Melatonin for the prevention and treatment of cancer, *Oncotarget* 8 (2017) 39896–39921. <https://doi.org/10.18632/oncotarget.16379>.
- [11] G.A. Bubenik, Gastrointestinal melatonin: Localization, function, and clinical relevance, *Dig. Dis. Sci.* 47 (2002) 2336–2348. <https://doi.org/10.1023/a:1020107915919>.
- [12] J. Liu, F. Huang, H.W. He, Melatonin effects on hard tissues: Bone and tooth, *Int. J. Mol. Sci.* 14 (2013) 10063–10074. <https://doi.org/10.3390/ijms140510063>.
- [13] P. Zrazhevskiy, M. Sena, X. Gao, Designing multifunctional quantum dots for bioimaging, detection, and drug delivery, *Chem. Soc. Rev.* 39 (2010): 4326–4354. <https://doi.org/10.1039/b915139g>.
- [14] P. Lissoni, F. Paolorossi, G. Tancini, A. Ardizzoia, S. Barni, F. Brivio, et al., A phase II study of tamoxifen plus melatonin in metastatic solid tumour patients, *Br. J. Cancer* 74 (1996) 1466–1468. <https://doi.org/10.1038/bjc.1996.566>.
- [15] S. Sun, H. Zeng, Size-controlled synthesis of magnetite nanoparticles, *J. Am. Chem. Soc.* 124 (2002) 8204–8205. <https://doi.org/10.1021/ja026501x>.
- [16] M. Martínez-Carmona, Y.K. Gun'ko, M. Vallet-Regí, Mesoporous silica materials as drug delivery: 'the nightmare' of bacterial infection, *Pharmaceutics* 10 (2018) 1–29. <https://doi.org/10.3390/pharmaceutics10040279>.
- [17] R. Sagayaraj, S. Aravazhi, G. Chandrasekaran, Review on structural and magnetic properties of (Co–Zn) ferrite nanoparticles, *Int. Nano Lett.* 11 (2021) 307–319. <https://doi.org/10.1007/s40089-021-00343-z>.
- [18] H. Li, Z. Kang, Y. Liu, S.-T. Lee, Carbon nanodots: synthesis, properties and applications, *J. Mater. Chem.* 22 (2012) 24230–24253. <https://doi.org/10.1039/C2JM34690G>.
- [19] L. Felicetti, M. Femminella, G. Reali, P. Liò, A Molecular Communication System in Blood Vessels for Tumor Detection, Association for Computing Machinery, New York, NY. (2014) 1–9. <https://doi.org/10.1145/2619955.2619978>.
- [20] V. Agrahari, P.-A. Burnouf, T. Burnouf, V. Agrahari, Nanoformulation properties, characterization, and behavior in complex biological matrices: Challenges and opportunities for brain-targeted drug delivery applications and enhanced translational potential, *Adv. Drug Deliv. Rev.* 148 (2019) 146–180. <https://doi.org/10.1016/j.addr.2019.02.008>.
- [21] N. Mozafari, N. Mozafari, A. Dehshahri, A. Azadi, Knowledge Gaps in Generating Cell-Based Drug Delivery Systems and a Possible Meeting with Artificial Intelligence, *Mol. Pharmaceutics* 20 (2023) 3757–3778. <https://doi.org/10.1021/acs.molpharmaceut.3c00162>.
- [22] H.C. Zhang, H. Ming, S. Lian, H. Huang, H. Li, et al., Fe<sub>2</sub>O<sub>3</sub> / carbon quantum dots complex photocatalysts and their enhanced photocatalytic activity under visible light, *Dalton Trans.* 40 (2011) 10822–10825. <https://doi.org/10.1039/C1DT11147G>.
- [23] S. Zhu, Y. Song, X. Zhao, J. Shao, J. Zhang, B. Yang, The photoluminescence mechanism in carbon dots (graphene quantum dots, carbon nanodots, and polymer dots): current state and future perspective, *Nano Res.* 8 (2015) 355–381. <https://doi.org/10.1007/s12274-014-0644-3>.
- [24] A. Carrillo-Vico, P.J. Lardone, N. Álvarez-Sánchez, A. Rodríguez-Rodríguez, J.M. Guerrero, Melatonin: Buffering the immune system, *Int. J. Mol. Sci.* 14 (2013) 8638–8683. <https://doi.org/10.3390/ijms14048638>.